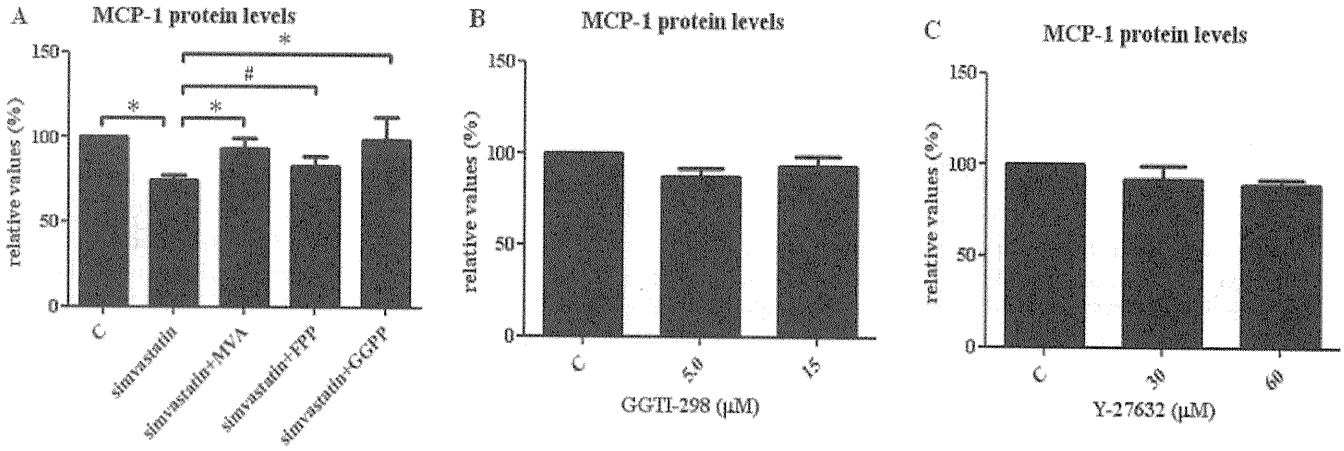

Fig. 4. Effects of MVA and isoprenoids on the simvastatin-mediated suppression of MCP-1 production by FLS.
A. MVA and GGPP attenuated suppression of MCP-1 production by simvastatin in RA FLS. FLS were incubated with 0.1–10 μM simvastatin for 24 h. MCP-1 levels in culture supernatants were determined by ELISA (n=6); $^{*}p<0.05$ versus control, $^{\#}$not significant. **B, C.** The production of MCP-1 was not affected by GGTI-298 (**B**, n=3) and Y-27632 (**C**, n=3).

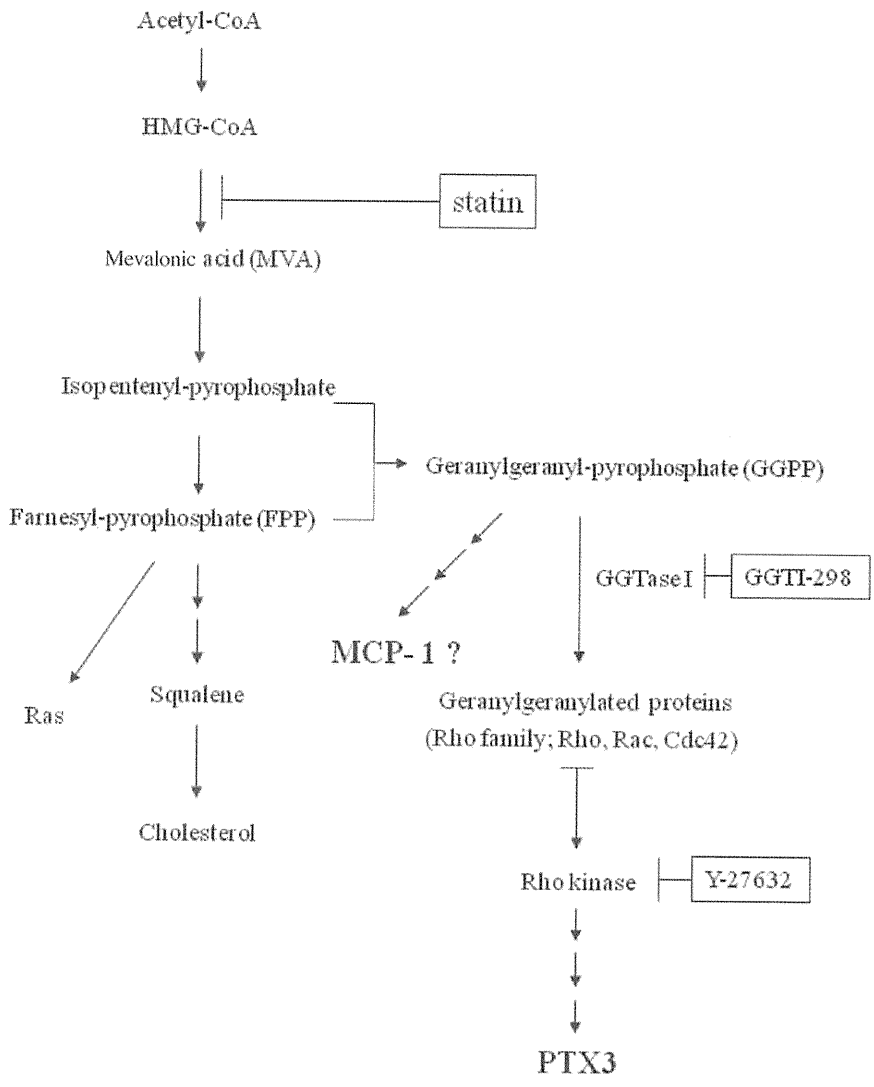

Fig. 5. Simvastatin affects FLS by two different mechanisms.
Simvastatin both reduced the secretion of PTX3 and MCP-1 in FLS. Whereas it inhibits PTX3 production in a Rho-dependent manner, it inhibits MCP-1 production in a Rho-independent manner.

on PTX3 production in the absence of simvastatin (data not shown).

Inhibitory effects of GGTI-298 and Y-27632 on PTX3 production in FLS

When FLS were incubated for 24 h with the GGTI-298, the PTX3 protein secreted into culture supernatants was reduced to 17.7±3.7% and 6.8±1.6% of control, with 5.0 μM and 15 μM GGTI-298, respectively (Fig. 2B). When FLS were incubated with Y-27632 for 24 h, PTX3 levels were reduced to 68.0±12.6% and 32.8±4.4% of control, with 30 μM and 60 μM Y-27632, respectively (Fig. 2C).

Inhibitory effects of simvastatin on MCP-1 production in RA FLS

So far, most of the molecules that we discovered to be reduced by simvastatin were regulated in a Rho-kinase dependent manner (16, 17). In our screening process, however, we also discovered a molecule, MCP-1, that was reduced by simvastatin in a Rho-kinase independent manner. The chemokine MCP-1 has been suggested to be a potential therapeutic target in RA. Its level increases in the peripheral blood, synovial fluid and synovial tissue in patients with RA, and it is known to be a potent chemoattractant for monocytes/macrophages and T cells (18).

As shown in Figure 3A, the levels of MCP-1 secreted by RA FLS after 24 h-culture in the absence of simvasta-

tin were significantly higher than those with OA.

When FLS from RA patients were incubated for 24 h with simvastatin, the MCP-1 levels in culture supernatants were reduced significantly, to 69.3±6.2%, 69.0±10.0% and 67.1±1.7%, compared with control, in the presence of 0.1 μM, 1.0 μM and 10 μM simvastatin, respectively (Fig. 3B). The expression of MCP-1 mRNA was also reduced to 62.6±15.1%, 61.0±9.3% and 56.2±9.7%, compared to controls, in the presence of 0.1 μM, 1.0 μM and 10 μM simvastatin, respectively (Fig. 3C).

MVA and GGPP restore the production of MCP-1 in FLS in the presence of simvastatin

As shown in Figure 4A, the inhibitory effect of 1.0 μM simvastatin on MCP-1 production in RA FLS attenuated if the cells were simultaneously treated by 100 μM MVA or 10 μM GGPP, but unaffected by FPP. MVA, GGPP and FPP had minimal effects on MCP-1 production in the absence of simvastatin (data not shown).

No inhibitory effects of GGTI-298 and Y-27632 on MCP-1 production in FLS

When FLS were incubated with GGTI-298 or Y-27632 for 24 h, the levels of MCP-1 were not affected by these reagents in contrast to those of PTX3 (Fig. 4B).

Discussion

In our previous reports, the production of IL-6 and IL-8 was also found to be regulated by the GGPP-dependent pathway (16). Since the expression of IL-6, IL-8 and MCP-1 in RA synovium appears to be associated with disease activity (19, 20, 21), simvastatin is thought to act via these pathways to show beneficial effects on RA patients. Furthermore, it has been demonstrated that MCP-1 is stored and released from vesicles in FLS and that high density lipoproteins (HDL) inhibit the release of MCP-1 (22). Since statins are known to increase the level of plasma HDL (23), simvastatin may inhibit both the production and release of MCP-1 from FLS.

In the present study, we have shown that simvastatin inhibited the production of PTX3 and MCP-1 on FLS from patients with RA. In addition, we have demonstrated that GGPP prevents the simvastatin-induced inhibition of PTX3 and MCP-1 production, suggesting that GGPP is critical for PTX3 and MCP-1 production in these cells. In accordance with our previous reports (16, 17), we now provide an additional evidence that simvastatin has beneficial effects on activated FLS from patients with RA.

It has been shown that the main source of PTX3 in the synovium of RA patients is pannus, in which monocytes/macrophages, FLS and endothelial cells are rich (5). It is tempting to speculate that PTX3 participates in synovial membrane injury by amplifying complement-mediated tissue damage (3). Based on these reports, our result may imply that simvastatin could improve the synovial membrane injury in RA patients.

On the other hand, among chemokines, MCP-1 is known to be a potent mediator for recruiting monocytes/macrophages and T cells (24). These cells have been shown to be directly involved in the induction and perpetuation of synovitis and subsequent joint destruction in RA (21). It has been shown that arthritis in MRL/*lpr* mice is suppressed by treating with anti-MCP-1 monoclonal antibodies before the disease-onset (25). Several lines of evidence have suggested MCP-1 plays important roles in monocyte recruitment and developing atherosclerosis (26, 27). Taken together with a poor-prognostic link between atherosclerosis and RA (28), MCP-1 may be one of the target molecules in the treatment of RA from both an anti-inflammatory and an anti-atherosclerotic aspects. Thus, simvastatin could reduce not only cardiovascular morbidity and mortality but also improve clinical measures in RA patients.

Surprisingly, treating FLS with GGTI-298 or Y-27632 significantly inhibited the production of PTX3, but had no effect on MCP-1 production. We speculated that Rho/Rho kinase may be involved in regulating the production of PTX3 but not MCP-1 in FLS (Fig. 5). In fact, it has been reported that in human endothelial cells and macrophages, statins inhibit CCR2/MCP-1 receptor expression via Rho-independent pathway (29). Therefore, in FLS it is possible that simvastatin inhibits the production of MCP-1 via Rho-independent pathway.

In conclusion, although simvastatin inhibits both PTX3 and MCP-1 production in RA FLS, the mechanisms are quite different. Simvastatin inhibits PTX3 production in a Rho-dependent manner but MCP-1 production in a Rho-independent manner. Understanding the multiple mechanisms by which simvastatin reduces these inflammatory mediators, we may be able to finely regulate the pathological conditions of patients with rheumatic diseases, such as RA.

Acknowledgements

We thank Dr Hiromi Oda and Dr Yoon Taek Kim, Department of Orthopaedic Surgery, Saitama Medical University, for providing synovial tissues, and Ms Toshiko Ishibashi and Ms Mina Sagara for technical assistance.

References

1. GARLANDA C, BOTTAZZI B, BASTONE A, MANTOVANI A: Pentraxins at the crossroads between innate immunity, inflammation, matrix deposition, and female fertility. *Annu Rev Immunol* 2005; 23: 337-66.
2. BREVIARIO F, D'ANIELLO EM, GOLAY J *et al.*: Interleukin-1-inducible genes in endothelial cells. Cloning of a new gene related to C-reactive protein and serum amyloid P component. *J Biol Chem* 1992; 267: 22190-7.
3. ORTEGA-HERNANDEZ OD, BASSI N, SHOENFELD Y, ANAYA JM: The Long Pentraxin 3 and Its Role in Autoimmunity. *Semin Arthritis Rheum* 2009; 39; 38-54.
4. PEPYS MB, HIRSCHFIELD GM: C-reactive protein: a critical update. *J Clin Invest* 2003; 111: 1805-12.
5. LUCHETTI MM, PICCININI G, MANTOVANI A *et al.*: Expression and production of the long pentraxin PTX3 in rheumatoid arthritis (RA). *Clin Exp Immunol* 2000; 119: 196-202.
6. MARON DJ, FAZIO S, LINTON MF: Current perspectives on statins. *Circulation* 2000; 101: 207-13.
7. STOSSEL TP: The discovery of statins. *Cell* 2008; 134: 903-5.
8. KWAK B, MULHAUPT F, MYIT S, MACH F: Statins as a newly recognized type of immunomodulator. *Nat Med* 2000; 6: 1399-402.
9. WEITZ-SCHMIDT G, WELZENBACH K, BRINKMANN V *et al.*: Statins selectively inhibit leukocyte function antigen-1 by binding to a novel regulatory integrin site. *Nat Med* 2001; 7: 687-92.
10. TAKEMOTO M, LIAO JK: Pleiotropic effects of 3-hydroxy-3-methylglutaryl coenzyme

a reductase inhibitors. *Arterioscler Thromb Vasc Biol* 2001; 21: 1712-9.
11. VAN AELST L, D'SOUZA-SCHOREY C: Rho GTPases and signaling networks. *Genes Dev* 1997; 11: 2295-322.
12. VOGT A, SUN J, QIAN Y, HAMILTON AD, SEBTI SM: The geranylgeranyltransferase-I inhibitor GGTI-298 arrests human tumor cells in G0/G1 and induces p21(WAF1/CIP1/SDI1) in a p53-independent manner. *J Biol Chem* 1997; 272: 27224-9.
13. MATOZAKI T, NAKANISHI H, TAKAI Y: Small G-protein networks: their crosstalk and signal cascades. *Cell Signal* 2000; 12: 515-24.
14. KANDA H, HAMASAKI K, KUBO K *et al.*: Antiinflammatory effect of simvastatin in patients with rheumatoid arthritis. *J Rheumatol* 2002; 29: 2024-6.
15. KANDA H, YOKOTA K, KOHNO C *et al.*: Effects of low-dosage simvastatin on rheumatoid arthritis through reduction of Th1/Th2 and CD4/CD8 ratios. *Mod Rheumatol* 2007; 17: 364-8.
16. YOKOTA K, MIYAZAKI T, HIRANO M, AKIYAMA Y, MIMURA T: Simvastatin inhibits production of interleukin 6 (IL-6) and IL-8 and cell proliferation induced by tumor necrosis factor-alpha in fibroblast-like synoviocytes from patients with rheumatoid arthritis. *J Rheumatol* 2006; 33: 463-71.
17. YOKOTA K, MIYOSHI F, MIYAZAKI T *et al.*: High concentration simvastatin induces apoptosis in fibroblast-like synoviocytes from patients with rheumatoid arthritis. *J Rheumatol* 2008; 35: 193-200.
18. LOETSCHER P, SEITZ M, CLARK-LEWIS I, BAGGIOLINI M, MOSER B: Monocyte chemotactic proteins MCP-1, MCP-2, and MCP-3 are major attractants for human CD4+ and CD8+ T lymphocytes. *FASEB J* 1994; 8: 1055-60.
19. BROZIK M, ROSZTÓCZY I, MERÉTEY K *et al.*: Interleukin 6 levels in synovial fluids of patients with different arthritides: correlation with local IgM rheumatoid factor and systemic acute phase protein production. *J Rheumatol* 1992; 19: 63-8.
20. KRAAN MC, PATEL DD, HARINGMAN JJ *et al.*: The development of clinical signs of rheumatoid synovial inflammation is associated with increased synthesis of the chemokine CXCL8 (interleukin-8). *Arthritis Res* 2001; 3: 65-71.
21. HARIGAI M, HARA M, YOSHIMURA T, LEONARD EJ, INOUE K, KASHIWAZAKI S: Monocyte chemoattractant protein-1 (MCP-1) in inflammatory joint diseases and its involvement in the cytokine network of rheumatoid synoviun. *Clin Immunol Immunopathol* 1993; 69: 83-91.
22. SCANU A, OLIVIERO F, GRUAZ L *et al.*: High-density lipoproteins downregulate CCL2 production in human fibroblast-like synoviocytes stimulated by urate crystals. *Arthritis Res Ther* 2010; 12: R23.
23. NICHOLLS SJ, TUZCU EM, SIPAHI I *et al.*: Statins, high-density lipoprotein cholesterol, and regression of coronary atherosclerosis. *JAMA* 2007;297:499-508.
24. ROLLINS BJ: Chemokines. *Blood* 1997; 90: 909-28.
25. GONG JH, RATKAY L G, WATERFIELD JD, CLARK-LEWIS I: An antagonist of monocyte chemoattractant protein 1 (MCP-1) inhibits arthritis in the MRL-lpr mouse model. *J Exp Med* 1997; 186: 131-7.
26. PIEMONTI L, CALORI G, LATTUADA G *et al.*: Association between plasma monocyte chemoattractant protein-1 concentration and cardiovascular disease mortality in middle-aged diabetic and nondiabetic and nondiabetic individuals. *Diabetes Care* 2009; 32: 2105-10.
27. SHANTSILA E, LIP GY: Monocytes in acute coronary syndromes. *Arterioscler Thromb Vasc Biol* 2009; 29: 1433-8.
28. BJÖRNÅDAL L, BRANDT L, KLARESKOG L, ASKLING J: Impact of parental history on patients› cardiovascular mortality in rheumatoid arthritis. *Ann Rheum Dis* 2006; 65: 741-5.
29. VEILLARD NR, BRAUNERSREUTHER V, ARNAUD C *et al.*: Simvastatin modulates chemokine and chemokine receptor expression by geranylgeranyl isoprenoid pathway in human endothelial cells and macrophages. *Atherosclerosis* 2006; 188: 51-8.

Mod Rheumatol (2010) 20:183–187
DOI 10.1007/s10165-009-0244-3

CASE REPORT

Analysis of cytokine production patterns of peripheral blood mononuclear cells from a rheumatoid arthritis patient successfully treated with rituximab

Akinori Yamamoto · Kojiro Sato · Fumihiko Miyoshi · Yasufumi Shindo · Yoshihiro Yoshida · Kazuhiro Yokota · Kyoichi Nakajima · Haruhiko Akiba · Yu Asanuma · Yuji Akiyama · Toshihide Mimura

Received: 11 March 2009 / Accepted: 1 October 2009 / Published online: 7 November 2009

Abstract We had a rheumatoid arthritis (RA) patient resistant to multiple drugs and who developed panniculitis due to etanercept treatment, then responded fairly well to rituximab. Intracellular staining of cytokines in the peripheral blood mononuclear cells before and after rituximab administration revealed that the cytokine production, representative of T-helper (Th)1-, Th2-, and Th17-type responses, decreased abruptly after the treatment. Interestingly, this timing coincided with that of the manifestation of the beneficial effect. This relationship may provide useful insight into the mechanism of action of the drug and hence about the pathogenesis of RA.

Keywords Rheumatoid arthritis · Rituximab · Th1 · Th2 · Th17

Introduction

Recently, with the advent of the so-called "biologics," the treatment of rheumatoid arthritis (RA), the most common autoimmune disease that affects and destroys joints, has undergone dramatic change. Biologics ameliorate the symptoms of RA that cannot be controlled by conventional disease-modifying antirheumatic drugs (DMARDs) and improve the patients' activities of daily living (ADL). Tumor necrosis factor (TNF) blockers spearheaded such new drugs [1, 2]. In 2008, the anti-interleukin (IL)-6 receptor antibody tocilizumab was also approved as a drug against RA in Japan [3, 4]. Furthermore, a fusion protein composed of an immunoglobulin (Ig) fused to the extracellular domain of CTLA-4 (abatacept [5]) and a monoclonal antibody against CD20, which is expressed on B cells (ocrelizumab [6]), are now undergoing clinical trials in Japan. In Europe and the USA, an anti-CD20 monoclonal antibody (rituximab [7]) and abatacept have already been approved. It is claimed that treatment with rituximab may be better for patients who exhibit an inadequate response to at least one anti-TNF agent rather than switching to an alternative anti-TNF agent [8]. Rituximab was first approved for B-cell non-Hodgkin's lymphoma, and the reason it is effective in treating RA remains unclear. Here we report a case of RA with effect attenuation of and/or intolerance to anti-TNF agents that was treated successfully with rituximab.

CD4-positive ($CD4^+$) effector T cells are typically divided into three subsets: Th1, Th2, and Th17 cells [9, 10]. Each subset plays a definitive role in the immune response. Th1 cells are mainly involved in cellular immunity, and Th2 cells are implicated in humoral immunity, including the allergic response. Th17 cells, recently identified, are considered to play important roles in certain autoimmune diseases, including RA and multiple sclerosis (MS). These subsets produce specific cytokines, and interferon gamma (IFN-γ), interleukin (IL)-4, and IL-17 are the representative cytokines of each subset. As Th17 cells have been implicated in the pathogenesis of RA, we performed a time-series assessment of the cytokine production pattern of $CD4^+$ T cells in peripheral blood mononuclear cells (PBMCs) from the patient in order to shed light on the mechanism(s) of action of rituximab in RA treatment.

A. Yamamoto · K. Sato (✉) · F. Miyoshi · Y. Shindo · Y. Yoshida · K. Yokota · K. Nakajima · H. Akiba · Y. Asanuma · Y. Akiyama · T. Mimura
Department of Rheumatology and Applied Immunology, Faculty of Medicine, Saitama Medical University Hospital, 38 Morohongo, Moroyama, Iruma-gun, Saitama 350-0495, Japan
e-mail: satok@saitama-med.ac.jp

Case report

A 64-year-old woman who had been diagnosed with RA 13 years ago and treated with various conventional DMARDs such as bucillamine, salazosulfapyridine, leflunomide (20 mg/day), and methotrexate (MTX, 2–4 mg/week) was admitted to our hospital because of severe arthritis and painful nodules under the skin. Infliximab (180 mg, along with MTX) had been introduced a year earlier but was stopped because of the attenuation of effect and the occurrence of shingles. Etanercept was then administered with good results. About 1 year later, however, numerous subcutaneous nodules with accompanying pain appeared on her limbs and trunk. Consequently, she was referred to this hospital and admitted for further examination. She had a brother and a sister who were also afflicted with RA. On examination, the patient looked ill. Her temperature was 36.4°C, pulse 80 beats per minute, and blood pressure 170/98 mmHg. Her weight was 54.6 kg and height 150 cm. Chest sounds were normal. The abdomen was flat and soft, and bowel sounds were normal. Ulnar drift deformity of the fingers was observed bilaterally. Both shoulder joints, the left elbow joint, and both ankle joints were swollen and tender. Numerous tender nodules 1–2 cm in diameter were noted under the skin of the limbs and the trunk; some of them accorded with the sites of etanercept injection. Erythrocyte sedimentation rate (ESR) was 57 mm/h, C-reactive protein (CRP) level <0.10 mg/dl, rheumatoid factor (RF) 419 IU/ml, and matrix metalloproteinase-3 (MMP-3) 534.2 ng/ml. The Disease Activity Score of 28 joints (DAS28)-CRP4 level was 6.3 and DAS28-ESR4 7.46. CRP level was not high, probably because of etanercept treatment until just before the admission. Functional class was estimated to be class III and radiographic stage was assessed as stage II. Infectious conditions including cutaneous tuberculosis were unlikely in light of negative tuberculin test and other cultivation tests. Skin biopsy was performed and revealed diffuse changes in subcutaneous adipose tissue with the infiltration of inflammatory cells, mostly lipophages, indicating a chronic lobular panniculitis. No vasculitis was present. A side effect of etanercept was suspected, and the skin lesions subsided gradually after cessation of the agent.

The arthralgia, however, became poorly controlled. Despite the increased dose of glucocorticoid (betamethasone 1.0 mg/day to 2.0 mg/day), inflammatory maker levels were gradually elevated and settled at as high as 10 mg/dl for CRP and 100 mm/h for ESR. DAS28 also increased and reached 6.21 (CRP4) and 7.27 (ESR4) 4 month after admission. She became almost bedridden because of arthralgia. By that time, tacrolimus, MTX, and salazosulfapyridine had been tried one after another in turn but had to be stopped because of side effects (deterioration in renal function, abdominal and dorsal eruption, and fever and eruption, respectively). To relieve the pain, glucocorticoid injection was performed almost every 2 weeks (8 mg of dexamethasone sodium phosphate intra-articularly, 4 mg of dexamethasone palmitate intravenously, or 40 mg triamcinolone acetonide intra-articularly), without lasting effect (Fig. 1a).

Finally, we decided to use rituximab because there was no other biologic available at that time (in 2007). After obtaining permission of the medical ethics board at this hospital, 500 mg of rituximab was administered intravenously twice in 2 weeks. Ibuprofen (200 mg) and DL-chlorpheniramine maleate (2 mg) were administered orally and hydrocortisone sodium succinate (100 mg) intravenously as prophylactic medication. Except for flushing of the face, no apparent injection reaction was observed. Before the second injection, the number of B cells ($CD19^+$ cells) in the peripheral blood dropped from 150/μl to <10/μl. This decrease was irrespective of the expression of an activation marker CD38 (Fig. 1b). For approximately 1 month after the treatment, no improvement was detected either subjectively or objectively. After that, however, the level of CRP decreased to <0.1 mg/dl fairly abruptly, and levels of ESR and RF were reduced also, although more gradually (Fig. 1a).

The numbers of $CD4^+$ and $CD8^+$ T cells in the peripheral blood were not significantly affected by rituximab. To estimate the pattern of Th response before and after rituximab treatment, we performed flow cytometric analysis of intracellular cytokines, namely, IFN-γ, IL-4, and IL-17, in $CD4^+$ cells (Fig. 2). PBMCs were separated by a centrifugation method using Ficoll–Conray solution (Lymphosepal, Immuno-Biological Laboratories, Japan). PBMCs were cultured in the Roswell Park Memorial Institute (RPMI) 1640 medium supplemented with 10% fetal bovine serum (FBS) in the presence of phorbol myristate acetate (PMA, 40 ng/ml) and ionomycin (1 μg/ml) for 5 h. During the last 1 h, monensin [Golgistop, Becton, Dickinson (BD) Bioscience, USA] was added to the culture. After that, cells were stained with anti-CD4- phycoerythrin/cytochrome 5 (PE/Cy5), and intracellularly stained with anti-IFN-γ fluorescein isothiocyanate (FITC) and either anti-IL-4-PE or anti-IL-17-PE (all reagents were from BD Bioscience). The cells were then analyzed using a FACSCan (BD Bioscience). Interestingly, the rate of cytokine-positive cells dropped suddenly 1 month after the treatment. The decrease in the number of IL-4-positive cells was the greatest: >90%. IL-17- or IFN-γ-positive cells were decreased by approximately 80% and 40%, respectively. The levels of IL-4 and IL-17 detected in the supernatant of the cells stimulated in vitro (without the addition of monensin) also dropped drastically, although that of IFN-γ did not decrease significantly (data not

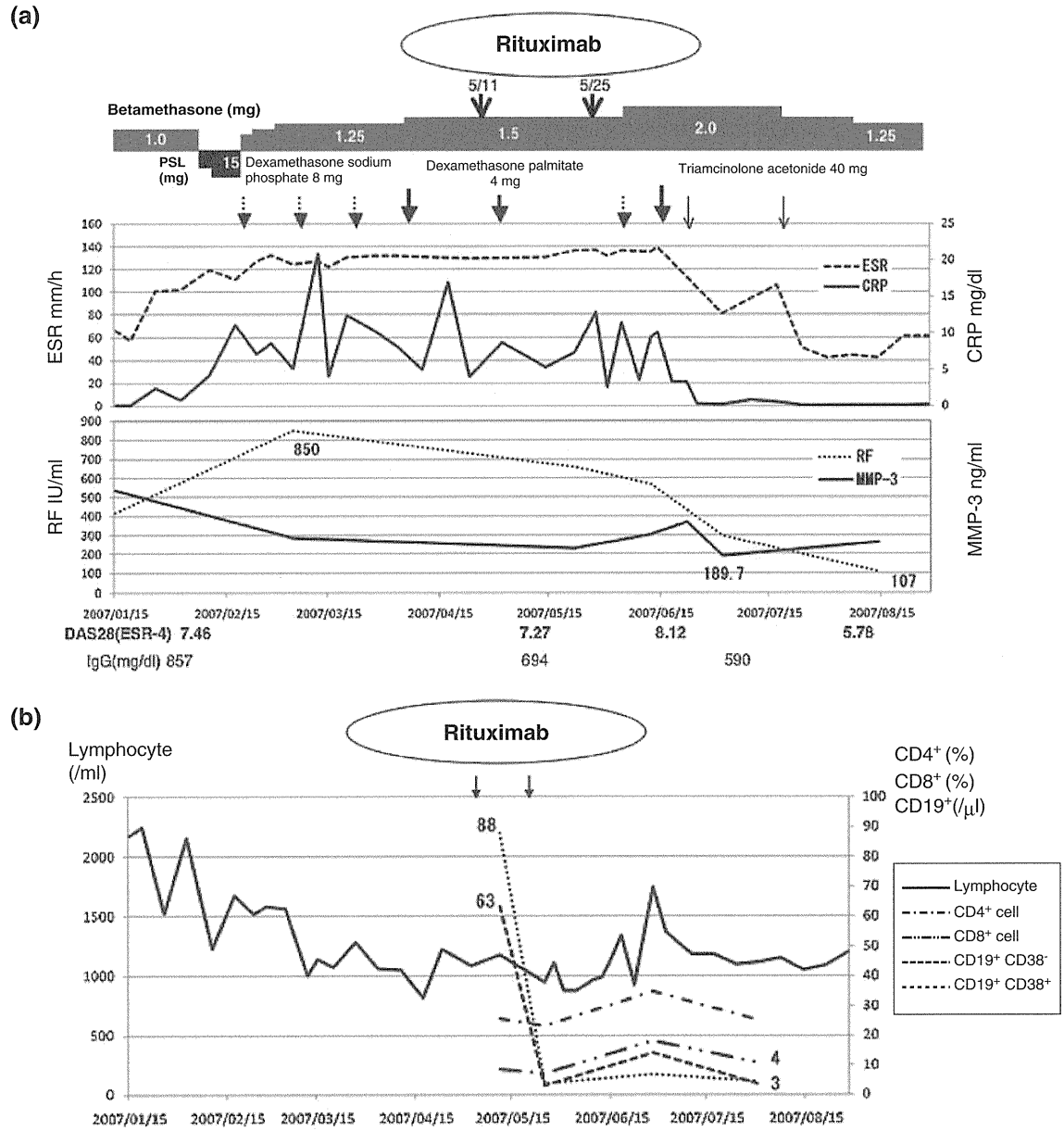

Fig. 1 Clinical course of the patient (**a**) and time course of the numbers of total lymphocytes, $CD19^{+}CD38^{+}$ B cell, and $CD19^{+}CD38^{-}$ B cell (/μl), and the ratio of $CD4^{+}$ and $CD8^{+}$ cells (%) in the peripheral blood (**b**). Although rituximab dramatically reduced the number of circulating B cells, it did not significantly affect the number of $CD4^{+}$ and $CD8^{+}$ cells. *PSL* prednisolone

shown). Thus, although the decrease in the rate (and fluorescence intensity) of IFN-γ-positive cells may have little significance, those of IL-4- and IL-17-positive cells are likely to be functionally significant. Two months after the treatment, the rates of cytokine-positive cells returned to nearly the former values. Four months after the treatment, the number of B cells remained low, and the levels of CRP and ESR were <0.10 mg/dl and 22 mm/h, respectively, regardless of the fact that we tapered the dose of betamethasone to 1.5 mg. DAS28 at the time of discharge was 4.69 (CRP4) and 5.97 (ESR4); the patient's subjective symptoms did not improve much, although her objective symptoms, including joint swelling and warmth, had subsided greatly. She was followed at the previous clinic and about 1 year after the second injection of rituximab, she began to be treated with adalimumab (40 mg/2 weeks). It was tolerated well and proved effective in maintaining her ADL thereafter.

Discussion

The effects of rituximab on this patient have two outstanding characteristics. First, the effects were rather slow

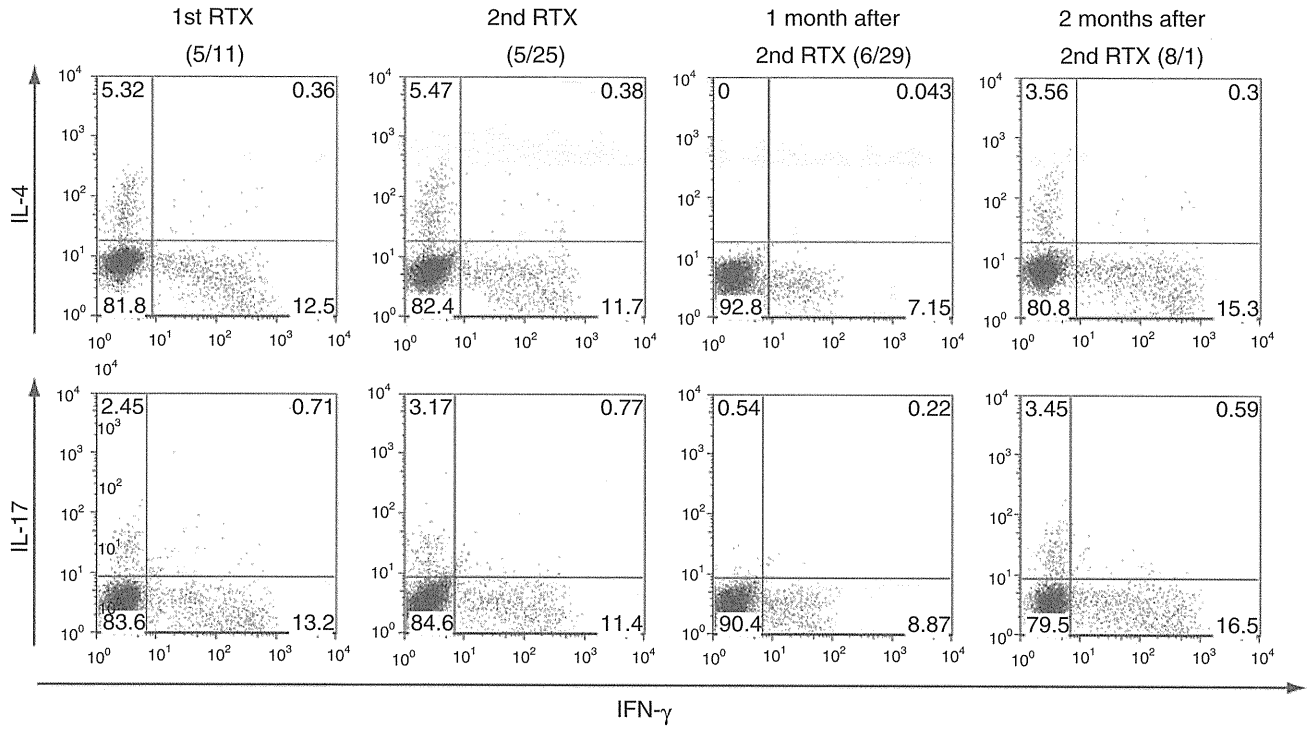

Fig. 2 Flow cytometric analysis of the intracellular cytokines in $CD4^+$ peripheral blood mononuclear cells (PBMCs) derived from the patient. Compared with data on the first day (11 May) of rituximab (RTX) treatment, the frequency of cytokine-positive cells was decreased significantly 1 month after the second RTX treatment (29 June)

to appear; it took almost 1 month for inflammatory markers to start dropping. This result is consistent with the report by Edwards et al. [7] and stands in striking contrast to the rapid onset of TNF blockers such as infliximab [11]. Cambridge et al. [12] reported that with rituximab treatment, Ig levels do not drop significantly, whereas those of anticyclic citrullinated peptide antibody (anti-CCP Ab) and RF dropped significantly but gradually. Autoantibodies increased just after the recovery of B cell number, and then the symptoms of RA relapsed. As CRP level decrease preceded that of the autoantibodies, however, the decrease of autoantibody levels might be interpreted not as a cause of but rather as a result of RA amelioration. Consistent with this, the transfer of large amounts of serum from patients with active RA, which contained RF, failed to induce any disease in the recipients, suggesting that antibodies including RF do not represent major effector mechanisms in RA [13]. It was also reported that rituximab was effective not only in RF-positive patients but also in RF-negative patients [14]. These results suggest that it is not the antibodies produced by B cells, but rather, the B cells themselves that are implicated in the pathogenesis of RA. For example, B cells may function as antigen-presenting cells. Alternatively, they may be required for the formation of lymph-node-like structures observed in the synovium of RA joints [15].

From this perspective, it is interesting that cytokine production from Th cells in the peripheral blood of our patient dropped, transiently, about 1 month after rituximab treatment, just when the desirable effects of the agent became apparent (Fig. 2). As far as we know, this is the first report on the relationship between treatment of RA with rituximab and the Th-cytokine production profile. Although the number of Th cells in the peripheral blood did not change significantly during this period (Fig. 1b), the B cell–T cell axis is likely to play an important role in maintaining the pathological conditions of RA. Recently, Th17 cells have been implicated in the pathogenesis of certain autoimmune diseases, including RA and MS; however, the decrease in cytokine-producing cells was not IL-17 specific. Rather, the number of IL-4-producing cells dropped the most. Thus, judging from the PBMC data alone, the importance of Th17 cells in the pathogenesis of RA is obscure. Of course, it should be noted that these responses were observed in PBMCs, not at the specific site(s) where inflammation occurred. What is precisely happening in the affected joints remains an interesting issue that is open to investigation. As an anti-CD20 antibody called ocrelizumab, similar to rituximab, is now under evaluation in a clinical trial worldwide, including Japan, we expect to be able to analyze further the cytokine

production patterns of patients treated with ocrelizumab in the near future.

Conflict of interest statement None.

References

1. Elliott MJ, Maini RN, Feldmann M, Kalden JR, Antoni C, Smolen JS, et al. Randomised double-blind comparison of chimeric monoclonal antibody to tumour necrosis factor alpha (cA2) versus placebo in rheumatoid arthritis. Lancet. 1994;344:1105–10.
2. Moreland LW, Baumgartner SW, Schiff MH, Tindall EA, Fleischmann RM, Weaver AL, et al. Treatment of rheumatoid arthritis with a recombinant human tumor necrosis factor receptor (p75)-Fc fusion protein. N Engl J Med. 1997;337:141–7.
3. Nishimoto N, Yoshizaki K, Miyasaka N, Yamamoto K, Kawai S, Takeuchi T, et al. Treatment of rheumatoid arthritis with humanized anti-interleukin-6 receptor antibody: a multicenter, double-blind, placebo-controlled trial. Arthritis Rheum. 2004;50:1761–9.
4. Smolen JS, Beaulieu A, Rubbert-Roth A, Ramos-Remus C, Rovensky J, Alecock E, et al. Effect of interleukin-6 receptor inhibition with tocilizumab in patients with rheumatoid arthritis (OPTION study): a double-blind, placebo-controlled, randomised trial. Lancet. 2008;371:987–97.
5. Kremer JM, Genant HK, Moreland LW, Russell AS, Emery P, Abud-Mendoza C, et al. Effects of abatacept in patients with methotrexate-resistant active rheumatoid arthritis: a randomized trial. Ann Intern Med. 2006;144:865–76.
6. Genovese MC, Kaine JL, Lowenstein MB, Giudice JD, Baldassare A, Schechtman J, et al. Ocrelizumab, a humanized anti-CD20 monoclonal antibody, in the treatment of patients with rheumatoid arthritis: a phase I/II randomized, blinded, placebo-controlled, dose-ranging study. Arthritis Rheum. 2008;58:2652–61.
7. Edwards JC, Szczepanski L, Szechinski J, Filipowicz-Sosnowska A, Emery P, Close DR, et al. Efficacy of B-cell-targeted therapy with rituximab in patients with rheumatoid arthritis. N Engl J Med. 2004;350:2572–81.
8. Finckh A, Ciurea A, Brulhart L, Kyburz D, Moller B, Dehler S, et al. B cell depletion may be more effective than switching to an alternative anti-tumor necrosis factor agent in rheumatoid arthritis patients with inadequate response to anti-tumor necrosis factor agents. Arthritis Rheum. 2007;56:1417–23.
9. Sato K. Th17 cells and rheumatoid arthritis—from the standpoint of osteoclast differentiation. Allergol Int. 2008;57:109–14.
10. Weaver CT, Hatton RD, Mangan PR, Harrington LE. IL-17 family cytokines and the expanding diversity of effector T cell lineages. Annu Rev Immunol. 2007;25:821–52.
11. Lipsky PE, van der Heijde DM, St Clair EW, Furst DE, Breedveld FC, Kalden JR, et al. Infliximab and methotrexate in the treatment of rheumatoid arthritis. Anti-Tumor Necrosis Factor Trial in Rheumatoid Arthritis with Concomitant Therapy Study Group. N Engl J Med. 2000;343:1594–602.
12. Cambridge G, Leandro MJ, Edwards JC, Ehrenstein MR, Salden M, Bodman-Smith M, et al. Serologic changes following B lymphocyte depletion therapy for rheumatoid arthritis. Arthritis Rheum. 2003;48:2146–54.
13. Harris J, Vaughan JH. Transfusion studies in rheumatoid arthritis. Arthritis Rheum. 1961;4:47–55.
14. Cohen SB, Emery P, Greenwald MW, Dougados M, Furie RA, Genovese MC, et al. Rituximab for rheumatoid arthritis refractory to anti-tumor necrosis factor therapy: results of a multicenter, randomized, double-blind, placebo-controlled, phase III trial evaluating primary efficacy and safety at twenty-four weeks. Arthritis Rheum. 2006;54:2793–806.
15. Manzo A, Pitzalis C. Lymphoid tissue reactions in rheumatoid arthritis. Autoimmun Rev. 2007;7:30–4.

Cancer Chemother Pharmacol (2011) 67:237–241
DOI 10.1007/s00280-010-1445-3

SHORT COMMUNICATION

The small-molecule tyrosine kinase inhibitor nilotinib is a potent noncompetitive inhibitor of the SN-38 glucuronidation by human UGT1A1

Ken-ichi Fujita · Minako Sugiyama · Yuko Akiyama · Yuichi Ando · Yasutsuna Sasaki

Received: 22 June 2010 / Accepted: 20 August 2010 / Published online: 2 September 2010

Abstract
Purpose Inhibition of the UDP-glucuronosyltransferase (UGT) 1A1 by nilotinib was examined in vitro with SN-38 as a substrate, to estimate the possibility of drug–drug interaction of nilotinib with other medicines predominantly detoxified by UGT1A1.
Methods Inhibition of UGT1A1-catalyzed SN-38 glucuronidation by nilotinib was examined with human liver microsomes (HLM) and recombinant human UGT1A1 as enzyme sources. Inhibition constants (K_i) were estimated with kinetic analysis.
Results Nilotinib potently inhibited the SN-38 glucuronidation by human liver microsomal UGT1A1 and recombinant UGT1A1 in a noncompetitive manner, with K_i values of 0.286 ± 0.0094 and 0.079 ± 0.0029 μM, respectively. If a drug that serves as a substrate of UGT1A1 is administered with nilotinib, the area under the plasma concentration–time curve of a drug estimated by using these K_i values would be two times or higher than that without nilotinib, suggesting drug–drug interactions involving UGT1A1. These in vitro data and the prediction of drug–drug interaction are helpful for the clinical management of the nilotinib use.
Conclusion We found that nilotinib is a potent noncompetitive inhibitor of human UGT1A1 activity.

Keywords Nilotinib · UGT1A1 · Inhibition · Drug–drug interaction · SN-38

K. Fujita (✉) · M. Sugiyama · Y. Akiyama · Y. Sasaki
Department of Medical Oncology, International Medical Center, Comprehensive Cancer Center, Saitama Medical University, 1397-1 Yamane, Hidaka, Saitama 350-1298, Japan
e-mail: fujitak@saitama-med.ac.jp

K. Fujita · M. Sugiyama · Y. Akiyama · Y. Sasaki
Project Research Laboratory, Research Center for Genomic Medicine, Saitama Medical University, 1397-1 Yamane, Hidaka, Saitama 350-1241, Japan

Y. Ando
Department of Clinical Oncology and Chemotherapy, Nagoya University Hospital, 65 Tsurumai-Cho, Showa-Ku, Nagoya 466-8560, Japan

Introduction

Drug–drug interactions have received increasing attention over the past few decades. A recent survey indicated that more than 30% of the US population over 57 years of age takes at least five prescription drugs at any given time. Drug–drug interactions contributed to the toxicity of some drugs that were withdrawn from the US market. Many of these interactions involved inhibition of drug-metabolizing enzymes and transporters, resulting in increased systemic exposure and subsequent adverse drug reactions [1]. Therefore, the evaluation of drug–drug interaction potential is an essential part of risk assessment for the better clinical management of the use of medicines.

Nilotinib is a small-molecule multiprotein tyrosine kinase inhibitor, targeting the Bcr-Abl fusion protein, c-Kit, platelet-derived growth factor receptor (PDGFR) α, and PDGFR β [2, 3], which is approved for the treatment of Bcr-Abl positive CML in adult patients resistant to or intolerant of prior therapy that included imatinib [4]. One study has suggested that nilotinib might inhibit UDP-glucuronosyltransferase (UGT) 1A1 to cause hyperbilirubinemia [5]. If nilotinib is a potent inhibitor of UGT1A1, physicians should pay attention to the drug–drug interactions between nilotinib and other medicines that served as

substrate of UGT1A1. The inhibition of estradiol glucuronidation by nilotinib was previously studied in vitro (European Medicines Agency; http://www.ema.europa.eu/ema/index.jsp?curl=pages/home/Home_Page.jsp&murl=&mid=). However, there has been no report demonstrating the details of the in vitro study. Furthermore, there is no quantitative estimation of the nilotinib-induced drug–drug interactions with the K_i value obtained in the in vitro study.

Therefore, in the present study, we assessed the inhibition of UGT1A1 activity by nilotinib in vitro using SN-38 as a substrate. Human liver microsomes (HLM) and recombinant human UGT1A1 were used as the source of UGT1A1. We further quantitatively estimated the possibility of nilotinib-induced drug–drug interaction.

Methods

Chemicals

Nilotinib, SN-38, and SN-38 glucuronide (SN-38G) were purchased from Toronto Research Chemicals (North York, Canada). Camptothecin was from Wako (Tokyo, Japan). UGT reaction mix solution A (25 mM UDP-glucuronic acid [UDPGA] cofactor) and UGT reaction mix solution B (5×-UGT buffer mix with alamethicin, 250 mM Tris–HCl, 40 mM $MgCl_2$, and 0.125 mg/mL alamethicin in water) were from BD Biosciences (Woburn, MA). All chemicals and solvents were of the highest grade commercially available.

Human liver microsomes and recombinant human UGT1A1

Pooled HLM were purchased from BD Biosciences (Woburn, MA). The pooled HLM were derived from 24 donors (92% Caucasian, 4% Hispanic, and 4% African-American; 17 men and 7 women) with a median age of 45 years (range, 16–77). Microsomes were diluted in 250 mM sucrose. Microsomal protein content was 20 mg/mL. Estradiol 3-glucuronidation by the liver microsomes measured by BD Biosciences (Woburn, MA) was 720 pmol/min/mg prot. Recombinant human UGT1A1 supersomes expressed in baculovirus-infected insect cells were obtained from BD Biosciences (Woburn, MA). Microsomal protein content was 5.0 mg/mL.

Inhibition assay of SN-38 glucuronidation

Based on the linear relation between the human liver microsomal protein concentration and the reaction time versus the amount of metabolite formation, the protein content and the reaction time were set at 0.5 mg/mL and 5 min, respectively. In the case using the recombinant human UGT1A1 as an enzyme source, the protein content and the reaction time were at 0.2 mg/mL and 30 min, respectively.

The effects of nilotinib on SN-38 glucuronidation by HLM or the recombinant human UGT1A1 were assessed as follows: After preincubation of the incubation mixture with nilotinib or solvent dimethyl sulfoxide (DMSO) at 37°C for 5 min, the substrate SN-38 dissolved in 1% DMSO was added. Nilotinib was dissolved in DMSO. The final concentration of the solvent in the reaction mixture was 1.1%. SN-38 glucuronidation by HLM or recombinant human UGT1A1 was assayed using BD Biosciences (Woburn, MA) products, as described in the UGT reaction mix solution A or B protocol. The typical incubation mixture consisted of 50 mM Tris–HCl buffer (pH 7.5), 8 mM $MgCl_2$, 25 μg/mL alamethicin, 2 mM UDPGA, and microsomal fractions of human liver or the recombinant human UGT1A1 in a final volume of 0.2 mL. The reaction was terminated by adding a twofold volume of acetonitrile. Each assay was performed three times in duplicate.

HPLC analysis for SN-38 glucuronide

SN-38G was analyzed by HPLC using a computerized HPLC system (Hitachi model 7000 series, Hitachi, Tokyo, Japan) equipped with a TSK-gel ODS-120T analytical column (4.6 × 250 mm; 4 μm; TOSOH, Tokyo, Japan), as described elsewhere [6]. The mobile phase consisted of 75 mM ammonium acetate (pH 4.75) for solvent A and acetonitrile for solvent B. The metabolite was separated using a linear gradient of 85–65% solvent A, a time of 0–25 min, and a flow rate of 1.0 mL/min. The metabolite was quantified by comparing the HPLC peak area to that of the internal standard camptothecin. The lower limit of quantification was 0.49 nM for SN-38G. The intra- and inter-assay coefficients of variation at 4.0 nM were less than 4.2 and 12.2%, respectively.

Estimation of enzyme and inhibition kinetics

When the HLM were used to estimate the enzyme kinetics (K_m and V_{max}) of SN-38 glucuronidation by UGT1A1 or to determine the K_i of nilotinib for UGT1A1-catalyzed SN-38 glucuronidation, SN-38 concentrations ranged from 2.5 to 40 μM in the absence or presence of an inhibitor (0.125–1 μM). In the case of using the recombinant human UGT1A1, SN-38 concentrations ranged from 1.25 to 40 μM in the absence or presence of an inhibitor (0.025–0.2 μM).

Michaelis–Menten equation was fitted to data points to estimate the K_m and V_{max} values by nonlinear least-squares regression analysis, performed with GraphPad Prism version 5 software (GraphPad Software). The K_i values were also calculated by nonlinear regression analysis with

GraphPad Prism version 5 software (GraphPad Software), using the equations for competitive inhibition, noncompetitive inhibition, or mixed inhibition [7]. The type of inhibition was determined from the enzyme inhibition models fitted to the data. Goodness of fit to the inhibition models was estimated from the F statistics, R^2 values, parameter standard error estimates, and 95% confidence intervals. Kinetic constants (K_m, V_{max}, and K_i) were reported as the means ± standard error.

Results

Inhibition of UGT1A1 by nilotinib

The substrate concentration versus SN-38 glucuronidation plots in the presence or absence of nilotinib is shown in Fig. 1a. Apparent K_m and V_{max} were calculated to be 6.80 ± 0.32 μM and 110 ± 1.8 pmol/min/mg prot., respectively. Nilotinib inhibited the SN-38 glucuronidation by UGT1A1 in a noncompetitive manner (Fig. 1b). The Eadie-Hofstee plots of SN-38 glucuronidation showed linearity with an R^2 value of 0.96, indicating that SN-38 glucuronidation was catalyzed by a single enzyme of UGT1A1 expressed in the HLM (Fig. 1c). Nonlinear regression analysis also revealed noncompetitive inhibition with R^2 of 0.99 (Fig. 1a). The K_i value was estimated to be 0.286 ± 0.0094 μM (Fig. 1a).

Apparent inhibition kinetics of nilotinib toward UGT1A1-mediated SN-38 was further examined with the recombinant human UGT1A1. Apparent K_m and V_{max} were calculated to be 4.18 ± 0.19 μM and 85.6 ± 1.3 pmol/min/mg prot., respectively (Fig. 2a). The K_m value obtained with the recombinant UGT1A1 was almost similar to that with HLM. Nilotinib inhibited the SN-38 glucuronidation by UGT1A1 in a noncompetitive manner (Fig. 2b). Nonlinear regression analysis also demonstrated noncompetitive inhibition with R^2 of 0.98 (Fig. 2a). The K_i value was estimated to be 0.079 ± 0.0029 μM (Fig. 2a).

Estimation of nilotinib-induced drug–drug interaction through UGT1A1

Inhibition of UGT1A1 activity by nilotinib may cause drug–drug interactions involving UGT1A1-catalyzed metabolism. The increase in the area under the plasma concentration–time curve (AUC) of other drugs by nilotinib can be estimated by using the K_i values obtained in this study using the method described by Ito et al. [8]. The average systemic plasma concentration of nilotinib after repeated oral administration ($[I]_{av}$) and the maximum unbound hepatic input concentration of nilotinib ($[I]_{in,u}$) are calculated as follows:

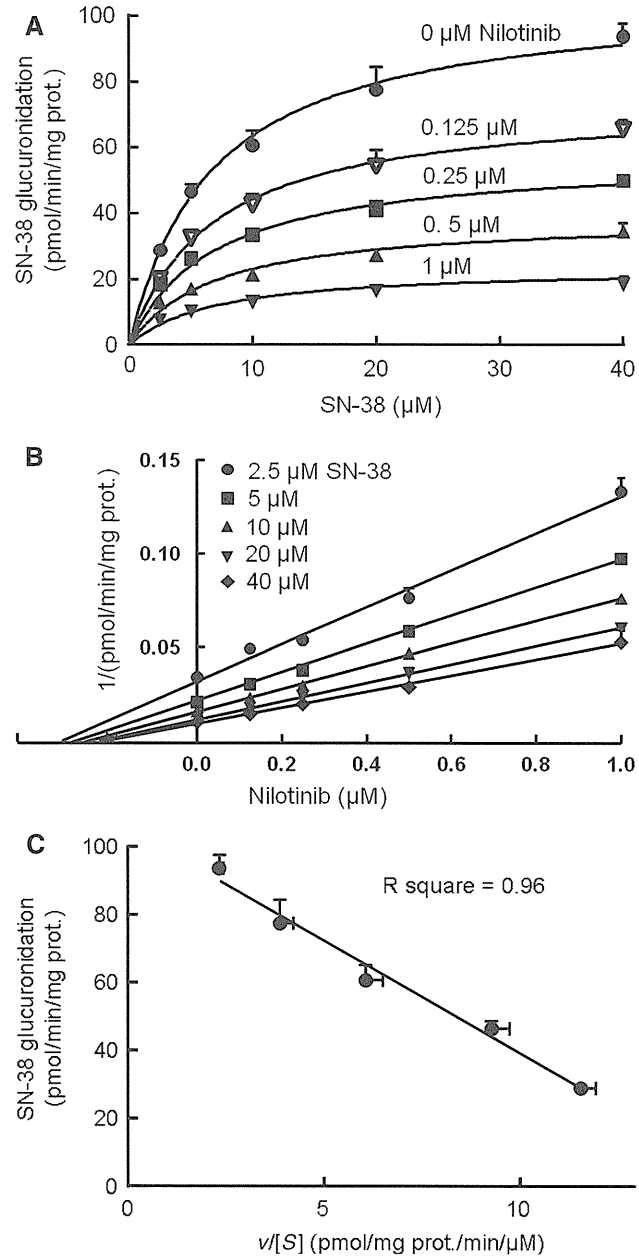

Fig. 1 Inhibition kinetics of nilotinib on SN-38 glucuronidation by UGT1A1 examined with human liver microsomes. **a** SN-38 concentration versus SN-38 glucuronidation plots. **b** Dixon plots. **c** Eadie-Hofstee plots of SN-38 glucuronidation in the absence of nilotinib. *v*, *Velocity* of glucuronidation; [*S*], SN-38 concentration. Each point shows the mean of three independent experiments with standard deviation

$$[I]_{av} = D/\tau/(CL/F) \quad (1)$$

$$[I]_{in,u} = fu\ ([I]_{av} + ka\ Fa D/Qh) \quad (2)$$

where D, τ, and CL/F are the dose, the dose interval and oral clearance of nilotinib, fu is the plasma unbound fraction, ka is the absorption rate constant, Fa is the extent of absorption, and Qh is the hepatic blood flow rate. The package inserts of nilotinib in the United States and Japan

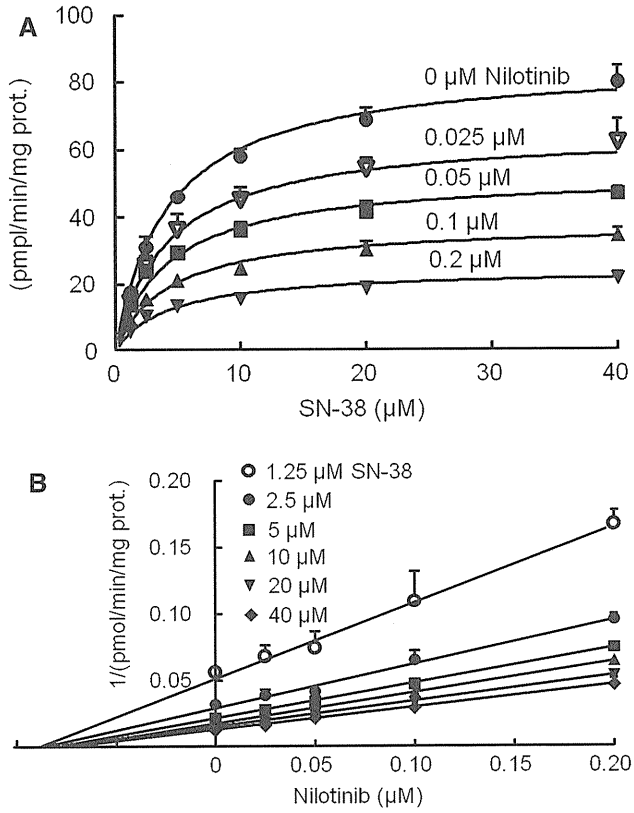

Fig. 2 Inhibition kinetics of nilotinib on SN-38 glucuronidation by recombinant human UGT1A1 **a** SN-38 concentration versus glucuronidation of SN-38. **b** Dixon plots. Each point represents the mean of three independent analyses with standard deviation

state that D and τ are 400 mg (0.685 mmol) and 12 h, respectively. CL/F obtained in fasting, Fa, and fu were reported to be 32.8 L/h, 0.3, and 0.02, respectively [9]. Since the ka value for nilotinib has not yet been reported, the value was assumed to be 0.1 min^{-1}, as proposed by Ito et al. [8]. The Qh was assumed to be 1,610 mL/min [8]. The AUC ratio in the presence or absence of nilotinib was used to estimate the potency of nilotinib to increase the AUC of a simultaneously administered drug that serves as a substrate of UGT1A1.

$$\text{AUC ratio} = 1 + [\text{I}]_{\text{in,u}}/K_i \quad (3)$$

The increase in the AUC was calculated to be 2.0 and 4.7 by using the K_i values obtained with HLM and recombinant human UGT1A1, respectively, even though we used the plasma unbound nilotinib concentration to reduce the possibility of false-positive estimates, suggesting the high risk of drug–drug interactions involving nilotinib [8].

Discussion

Our in vitro study showed that nilotinib was a potent noncompetitive inhibitor of human UGT1A1. The K_i values of UGT1A1 inhibition by nilotinib obtained with HLM and recombinant human UGT1A1 were 0.286 and 0.079 μM, respectively.

Singer et al. [5] suggested that the combined impact of the inhibition of UGT1A1 activity by nilotinib and genetic polymorphisms of *UGT1A1*, which were related to reduced expression or activity of UGT1A1, increased the incidence of hyperbilirubinemia. However, there has been no direct evidence on the inhibition of UGT1A1 by nilotinib [4, 5]. Our present results provide the first direct evidence for the in vitro inhibition of UGT1A1 activity by nilotinib and might support the mechanism of hyperbilirubinemia proposed by Singer et al. [5].

The increase in the AUC ratio of other drug to nilotinib was estimated to be higher than 2.0, suggesting the high risk of drug–drug interactions involving nilotinib [8]. Food intake has been shown to significantly affect the absorption of nilotinib [9]. Increased absorption of nilotinib was most pronounced after a high-fat meal, associated with an 82% increase in the AUC. Therefore, the AUC ratio may exceed 2.0, when nilotinib is taken after ingesting such foods. Caution should therefore be exercised when a drug serving as a substrate of UGT1A1 is administered with nilotinib.

The genetic polymorphisms in *UGT1A1* that cause lower expression of the protein (e.g., **28*) or lower catalytic activity of the enzyme (e.g., **6*) seen in patients with Gilbert's syndrome may further increase the AUC ratio as suggested by Singer et al. [5].

Interestingly, the FDA report [4] proposed that nilotinib competitively inhibited UGT1A1 activity, which does not agree with our findings. The reason for this difference is unclear because the FDA report did not include any experimental data.

Apparent K_m for SN-38 glucuronidation by UGT1A1 expressed in the HLM was concordant with the previous results [10]. V_{max} for the enzymatic reaction was about twice as high as that previously reported [10].

We compared the inhibition potency of SN-38 glucuronidation by nilotinib with several other small-molecule tyrosine kinase inhibitors. The lowest concentration that inhibited 50% of the maximal SN-38 glucuronidation by human UGT1A1 was obtained with nilotinib (0.146 μM), followed by sorafenib (0.446 μM), erlotinib (0.457 μM), lapatinib (1.47 μM), dasatinib (1.52 μM), gefitinib (3.50 μM), imatinib, and sunitinib (>10 μM). The results indicate that nilotinib is the most potent UGT1A1 inhibitor among small-molecule tyrosine kinase inhibitors tested.

We found that nilotinib is a potent noncompetitive inhibitor of UGT1A1. The result is applicable for the appropriate clinical management of the use of nilotinib with medicines predominantly metabolized by UGT1A1.

Acknowledgments We sincerely thank Drs. Yu, Sunakawa, Hiroo Ishida, Keishi Yamashita, Keiko Mizuno, Taro Yokoyama, Ken Shiozawa, Keisuke Miwa, Shigehira Saji, and Takashi Hirose for the valuable discussion on the present analyses. This study was supported in part by the Grant-in-Aid for Cancer Research 21S-8-1 from the Ministry of Health, Labour and Welfare of Japan, and in part by a grant-in-aid for "Support Project of Strategic Research Center in Private Universities" from the Ministry of Education, Culture, Sports, Science and Technology (MEXT) to Saitama Medical University Research Center for Genomic Medicine.

References

1. Zhang L, Reynolds KS, Zhao P, Huang SM (2010) Drug interactions evaluation: an integrated part of risk assessment of therapeutics. Toxicol Appl Pharmacol 243:134–145
2. Manley PW, Cowan-Jacob SW, Mestan J (2005) Advances in the structural biology, design and clinical development of Bcr-Abl kinase inhibitors for the treatment of chronic myeloid leukaemia. Biochim Biophys Acta 1754:3–13
3. Weisberg E, Manley P, Mestan J, Cowan-Jacob S, Ray A, Griffin JD (2006) AMN107 (nilotinib): a novel and selective inhibitor of BCR-ABL. Br J Cancer 94:1765–1769
4. Hazarika M, Jiang X, Liu Q, Lee SL, Ramchandani R, Garnett C, Orr MS, Sridhara R, Booth B, Leighton JK, Timmer W, Harapanhalli R, Dagher R, Justice R, Pazdur R (2008) Tasigna for chronic and accelerated phase Philadelphia chromosome–positive chronic myelogenous leukemia resistant to or intolerant of imatinib. Clin Cancer Res 14:5325–5331
5. Singer JB, Shou Y, Giles F, Kantarjian HM, Hsu Y, Robeva AS, Rae P, Weitzman A, Meyer JM, Dugan M, Ottmann OG (2007) UGT1A1 promoter polymorphism increases risk of nilotinib-induced hyperbilirubinemia. Leukemia 21:2311–2315
6. Araki K, Fujita K, Ando Y, Nagashima F, Yamamoto W, Endo H, Miya T, Kodama K, Narabayashi M, Sasaki Y (2006) Pharmacogenetic impact of polymorphisms in the coding region of the UGT1A1 gene on SN-38 glucuronidation in Japanese patients with cancer. Cancer Sci 97:1255–1259
7. Copeland RA (2000) Enzymes: a practical introduction to structure, mechanism, and data analysis. Wiley, New York
8. Ito K, Brown HS, Houston JB (2004) Database analyses for the prediction of in vivo drug-drug interactions from in vitro data. Br J Clin Pharmacol 57:473–486
9. Tanaka C, Yin OQ, Sethuraman V, Smith T, Wang X, Grouss K, Kantarjian H, Giles F, Ottmann OG, Galitz L, Schran H (2010) Clinical pharmacokinetics of the BCR-ABL tyrosine kinase inhibitor nilotinib. Clin Pharmacol Ther 87:197–203
10. Gagne JF, Montminy V, Belanger P, Journault K, Gaucher G, Guillemette C (2002) Common human UGT1A polymorphisms and the altered metabolism of irinotecan active metabolite 7-ethyl-10-hydroxycamptothecin (SN-38). Mol Pharmacol 62:608–617

JJCO Japanese Journal of Clinical Oncology

Jpn J Clin Oncol 2011;41(2)204–209
doi:10.1093/jjco/hyq197
Advance Access Publication 21 October 2010

Phase I/II Study of FOLFIRI in Japanese Patients with Advanced Colorectal Cancer

Keishi Yamashita[1], Fumio Nagashima[1,2], Ken-ichi Fujita[1,2,*], Wataru Yamamoto[1], Hisashi Endo[1], Toshimichi Miya[1], Masaru Narabayashi[1], Kaori Kawara[1], Yuko Akiyama[1,2], Yuichi Ando[1], Masahiko Ando[3] and Yasutsuna Sasaki[1,2]

[1]Department of Medical Oncology, International Medical Center-Comprehensive Cancer Center, Saitama Medical University, [2]Project Research Laboratory, Research Center for Genomic Medicine, Saitama Medical University, Hidaka, Saitama and [3]Department of Preventive Services, Kyoto University School of Public Health, Sakyo-ku, Kyoto, Japan

*For reprints and all correspondence: Ken-ichi Fujita, Department of Medical Oncology, International Medical Center-Comprehensive Cancer Center, Saitama Medical University, 1397-1 Yamane, Hidaka, Saitama 350-1298, Japan. E-mail: fujitak@saitama-med.ac.jp

Received August 5, 2010; accepted September 20, 2010

Objective: This phase I/II study determined the recommended dose of FOLFIRI (irinotecan, infusional 5-fluorouracil and leucovorin) for Japanese patients with advanced colorectal cancer, and evaluated safety at the recommended dose in patients without the *UDP-glucuronosyltransferase 1A1*28* allele which caused reduced enzyme expression.
Methods: The phase I part assessed the maximum tolerated dose of FOLFIRI to determine the recommended doses of irinotecan and infusional 5-fluorouracil. The doses were escalated from 150 to 180 mg/m^2 (irinotecan) and 2000 to 2400 mg/m^2 (5-fluorouracil). *UDP-glucuronosyltransferase 1A1*6* and **28*, and pharmacokinetics of irinotecan were observationally examined. In the phase II part, patients without the *UDP-glucuronosyltransferase 1A1*28* allele received FOLFIRI at the recommended dose to evaluate safety.
Results: Among 15 patients in the phase I part, dose-limiting toxicity (diarrhea) occurred in one patient who received 150 mg/m^2 irinotecan and 2400 mg/m^2 infusional 5-fluorouracil. The respective recommended doses were 180 and 2400 mg/m^2 for irinotecan and infusional 5-fluorouracil, without reaching the maximum tolerated dose. Twenty-five patients received FOLFIRI at the recommended doses. Grade 3 or 4 neutropenia occurred in 44%, and Grade 3 diarrhea in 4%.
Conclusions: This phase I/II study demonstrates that the recommended doses of irinotecan and infusional 5-fluorouracil in FOLFIRI for Japanese patients with advanced colorectal cancer who do not possess the *UDP-glucuronosyltransferase 1A1*28* allele are 180 and 2400 mg/m^2, respectively. Toxicities occurring at the recommended doses are manageable in these patients.

Key words: FOLFIRI – recommended dose – Japanese – safety – UGT1A1 genotyping

INTRODUCTION

FOLFIRI, infusional 5-fluorouracil (5-FU) and *l*-leucovorin (*l*-LV) plus irinotecan, was developed in Europe and is now widely used as one of the standard treatment regimens for advanced colorectal cancer (CRC) (1,2). The doses of irinotecan and infusional 5-FU in the FOLFIRI regimen used in Western countries are 180 mg/m^2 and 2400–3000 mg/m^2, respectively, repeated every 2 weeks (1,2). In Japanese patients, however, the maximum tolerated doses (MTD) of irinotecan and infusional 5-FU in FOLFIRI remain uncertain. We routinely use irinotecan at a dose of 150 mg/m^2 in FOLFIRI. This dose has been approved for irinotecan monotherapy every 2 weeks by the Japanese Ministry of Health, Labour and Welfare.

Several lines of evidence have linked irinotecan toxicity to the *UGT1A1*28* allele. Patients homozygous for *UGT1A1*28* carry a significantly higher risk of severe irinotecan-related adverse events than those who do not possess this genotype (3,4) because *UGT1A1*28* decreases UGT1A1 protein expression and reduces the glucuronidation capacity for SN-38. In Asians, a specific mutation, *UGT1A1*6* (5), has been proved to reduce the catalytic activity of UGT1A1 (6,7). The *UGT1A1*28/*28*, **6/*6* and **6/*28* genotypes have been shown to be related to severe neutropenia in Asian populations (8–10).

We performed a dose-finding phase I study of irinotecan and continuous infusional 5-FU in the FOLFIRI regimen in Japanese patients with advanced CRC. We also observationally examined the *UGT1A1* genotyping and irinotecan pharmacokinetics in the phase I part to investigate the relation between them and FOLFIRI-related toxicity. Then, we evaluated the safety and efficacy of FOLFIRI at the recommended dose (RD) in patients without the *UGT1A1*28* allele. Here, we report the results of the first Japanese phase I and II study of FOLFIRI with *UGT1A1* genotyping.

PATIENTS AND METHODS

Eligibility

This study enrolled patients with histologically confirmed advanced CRC. Eligibility criteria included an age of $\leq$75 years; an Eastern Cooperative Oncology Group (ECOG) scale performance status of 0 or 1; no previous chemotherapy for at least 4 weeks; no previous irinotecan-based chemotherapy; adequate bone marrow (absolute neutrophil count $\geq$2000/μl, platelet count $\geq$100 000/μl), liver [serum total bilirubin $\leq$ upper limit of normal (ULN), serum aspartate aminotransferase and alanine aminotransferase $\leq 3.0 \times$ ULN] and renal (serum creatinine $\leq 1.5 \times$ ULN) functions; no severe medical conditions; no brain metastasis and no prior radiotherapy of the pelvis. The Institutional Review Board of Saitama Medical University approved the study protocol. Patients signed written informed consent for their peripheral blood samples and medical information to be used for research purposes.

Study Objectives

Phase I Part

The primary objective of the phase I part of this study was to assess the MTD and dose-limiting toxicity (DLT) of irinotecan and infusional 5-FU in FOLFIRI during the first course of treatment in patients with advanced CRC and thereby determine the RD. *UGT1A1*28* and **6* and the pharmacokinetics of irinotecan, the active metabolite of irinotecan SN-38 and the inactive metabolite SN-38 glucuronide (SN-38G) were observationally examined to evaluate the relations of *UGT1A1* genotype to irinotecan pharmacokinetics and irinotecan-induced adverse events. Pharmacogenetic and pharmacokinetic information were not reflected for patient enrollment and dose escalation in the phase I part.

Phase II Part

In the subsequent phase II part of the study, we excluded patients who had at least one *UGT1A1*28* allele, because we had considered that these patients were at higher risk in irinotecan-induced severe toxicities based on the report by Ando et al. (3). The primary objective of the phase II part was to evaluate the safety of FOLFIRI at the RD. The secondary objective was to assess response.

Treatment and Dose Escalation

FOLFIRI comprised a 2-h intravenous infusion of *l*-LV (200 mg/m^2) and a 90-min intravenous infusion of irinotecan (each level as described below) on day 1, followed by an intravenous bolus injection of 5-FU (400 mg/m^2) and a 46-h intravenous infusion of 5-FU (each level as described below); treatment was repeated every 2 weeks. Two sessions of treatment were counted as one course. The starting doses (Level 1) of irinotecan and infusional 5-FU were 150 and 2000 mg/m^2, respectively. The dose of infusional 5-FU was increased to 2400 mg/m^2 (Level 2). Then, the doses of irinotecan and infusional 5-FU were elevated to 180 and 2400 mg/m^2, respectively (Level 3). If patients did not tolerate Level 1, the dose of irinotecan was decreased to 120 mg/m^2 (Level 0).

DLT was defined as Grade 4 neutropenia lasting for more than 5 days, neutropenic fever (Grade 3 or 4 neutropenia with fever $\geq$38.5°C), Grade 4 thrombocytopenia, Grade 3 thrombocytopenia with hemorrhage or Grade 3 or higher non-hematologic toxicity during the first course of treatment. Three patients were initially enrolled at each dose level. If none of the first three patients had DLT, the dose was escalated, and three additional patients received the next dose level. If one of the three patients had DLT, then three additional patients were enrolled at the same dose level, and escalation to the next dose level was continued if only one of the six patients had DLT. If DLT occurred in more than one of the first three patients or more than one of six patients treated at any given dose level, dose escalation was stopped, and that level was defined as MTD. If DLT occurred at dose Level 1, then the dose level was decreased to Level 0. If DLT occurred at dose Level 0, the study was stopped. Patients who received Level 0 and had DLT were treated with FOLFIRI at an irinotecan dose of 100 mg/m^2 (Level -1) after resolution of toxicity as evaluated by the physician in charge. In principle, the RD was defined as the dose one level below the MTD, but toxic effects occurring in later courses were also considered. Six patients were enrolled at the RD.

After determining the RD in the phase I part of the study, additional patients received FOLFIRI at the RD in the phase II part.

Toxicity was assessed weekly during the first course and every 2 weeks during the second and subsequent courses according to the National Cancer Institute Common Toxicity Criteria version 2.0 (http://ctep.cancer.gov/protocoldevelopment/electronic_applications/docs/ctcv20_4-30-992.pdf). Chemotherapy was delayed until recovery if the leukocyte count was $<3000/\mu l$, the platelet count was 100 000/μl or if clinically significant, persistent non-hematologic toxicity occurred. Tumor response was evaluated every two courses according to the standard World Health Organization response criteria (11). Treatment was continued until disease progression, unacceptable toxicity or the patient's refusal of further treatment.

UGT1A1 Genotyping

Genomic DNA was extracted from 200 μl of peripheral blood, which had been stored at −80°C until analysis, with the use of a QIAamp Blood Kit (QIAGEN GmbH, Hilden, Germany). The polymorphism *UGT1A1*6* was analyzed by the polymerase chain reaction-restriction fragment length polymorphism method as described elsewhere (12). *UGT1A1*28* was determined by the direct sequencing method as described by Fujita et al. (12).

Pharmacokinetic Analysis of Irinotecan and its Metabolites

Blood samples for pharmacokinetic analysis were obtained during the first treatment with FOLFIRI in the patients who agreed to have blood sampling for phamacokinetics. The samples were taken from the arm opposite the infusion site at the beginning of irinotecan infusion and at 0, 0.25, 0.5, 1, 2, 4, 8 and 24 h after the end of the 1.5 h infusion. The samples were immediately centrifuged, and the plasma was stored at −80°C until analysis. Total (lactone and carboxylate) plasma concentrations of irinotecan, SN-38 and SN-38G were analyzed by reverse-phase high-performance liquid chromatography as described by Araki et al. (8). The lower limits of quantification were 5 ng/ml (7.4 nM) for irinotecan and 0.5 ng/ml (1.2 and 0.88 nM) for SN-38 and SN-38G. The intra-assay and inter-assay coefficients of variation for irinotecan and its metabolites were $<10\%$.

Pharmacokinetic Parameters

The plasma concentration–time data of irinotecan and its metabolites were analyzed by a standard non-compartmental method, using WinNonlin version 5.2 software (Pharsight Corporation, Mountain View, CA, USA). The area under the plasma concentration–time curve (AUC) for time zero to the last sampling was calculated with the linear trapezoidal rule (until the peak plasma concentration) and linear-log trapezoidal rule (until the last quantifiable concentration).

Statistical Design in Phase II Part

In the phase II part of this study, we set a response rate of 25% as the target activity level and chose 5% as the lowest response rate of interest. According to Simon's two-stage minimax design with an α level of 10 and 90% power (13), we planned to enroll at least 20 patients at the RD, with at least one response among 13 patients in the first step being required for this regimen to be considered worthy of further evaluation. The exact confidence interval for the response rate was calculated based on binomial distribution.

RESULTS

Patient Characteristics

Between March 2005 and April 2007, a total of 34 patients were enrolled into this phase I/II study, 15 in phase I and 19 in phase II. The baseline characteristics of the patients are shown in Table 1. The median age was 61 years (range, 35–75). Twenty-three (67%) patients had received at least one prior regimen of chemotherapy.

Table 1. Baseline characteristics of all patients enrolled in the present phase I/II study

Characteristics	Number of patients
Age (years)	61 (35–75)[a]
Gender	
Male	21
Female	13
ECOG performance status	
0	31
1	3
Primary tumor	
Colon	21
Rectum	13
Number of metastases	
1	20
2	10
3	4
Number of prior chemotherapy regimens	
0	11
1	21
≥2	2

ECOG, Eastern Cooperative Oncology Group.
[a]Median (range).

Table 2. Dose escalation and dose-limiting toxicity in patients treated with FOLFIRI

Dose level	Irinotecan (mg/m^2)	5-FU (mg/m^2)	Toxicities[a]	*UGT1A1*		AUC (μM h)			$AUC_{SN-38}/AUC^{c}_{SN-38G}$
				**28*	**6*	Irinotecan	SN-38	SN-38G	
1	150	2000		−/−	+/−	—	—	—	—
				−/−	−/−	—	—	—	—
				−/−	−/−	—	—	—	—
2	150	2400		−/−	+/−	—	—	—	—
				−/−	−/−	7.27	0.36	0.41	0.89
				−/−	+/+	—	—	—	—
			Diarrhea (Grade 3)[b]	−/−	−/−	—	—	—	—
			Leukopenia/neutropenia (Grade 4)	+/−	+/−	9.76	1.06	0.49	2.16
				−/−	−/−	7.34	0.3	0.7	0.43
3	180	2400		−/−	−/−	8.15	0.7	0.5	1.39
				−/−	−/−	10.09	0.3	0.57	0.52
				−/−	−/−	13.4	0.72	1.79	0.4
				−/−	−/−	21.88	0.79	2.75	0.29
				−/−	−/−	—	—	—	—
				−/−	+/+	10.18	0.71	0.51	1.4

5-FU, 5-fluorouracil; AUC, area under the plasma concentration–time curve.
[a]Grade 4 hematologic and Grades 3–4 non-hematologic toxicities.
[b]This adverse event was dose-limiting toxicity.
[c]Ratio of AUC of SN-38 to AUC of SN-38G.

Phase I Part

The results of the phase I part are shown in Table 2. There was no DLT at dose Level 1. At dose Level 2, one of first three patients had leg edema diagnosed to be caused by deep vein thrombosis (DVT), initially designated as DLT. Three additional patients then received the same dose level. One patient had Grade 3 diarrhea. Although two of the first six patients who received dose Level 2 were initially judged to have DLT, further careful follow-up examinations of the patient considered to have DVT revealed no definite evidence of DVT; this reaction was therefore not considered DLT. We concluded that only one of the six patients given dose Level 2 had DLT and escalated the dose to Level 3. At dose Level 3, no DLT occurred in the first three patients. At that time, we obtained information regarding another ongoing phase I study of FOLFIRI in Japan. In that study, three of six patients who received irinotecan 180 mg/m^2 and infusional 5-FU 3000 mg/m^2 had DLT. This dose level was regarded to be the MTD, and the RD of irinotecan was determined to be the same as our dose Level 3 (14). On the basis of this information, we estimated that the RD was dose Level 3 and decided to confirm this by assigning three additional patients to this dose Level. None of the six patients given dose Level 3 had DLT. We therefore considered dose Level 3 the RD for the next phase II part of this study.

Among the 15 patients participating in the phase I study, the *UGT1A1* genotype was *UGT1A1*1/*1* in 10 patients, *UGT1A1*1/*6* in 2, *UGT1A1*6/*6* in 2 and *UGT1A1*6/*28* in 1. The patient with *UGT1A1*6/*28* genotype had Grade 4 neutropenia after receiving irinotecan at a dose of 150 mg/m^2. The pharmacokinetics of irinotecan, SN-38 and SN-38G were examined in eight patients. The average ratio of the AUC of SN-38 to that of SN-38G (AUC_{SN-38}/AUC_{SN-38G}) in the patients with *UGT1A1*6/*28* and *UGT1A1*6/*6* was 1.78. The average AUC_{SN-38}/AUC_{SN-38G} in the patients with *UGT1A1*1/*1* was 0.65.

Phase II Part

In the phase II part, we evaluated the safety and efficacy of FOLFIRI at the RD in 25 patients: 6 who received the RD in phase I and 19 who were newly enrolled. One patient was homozygous for *UGT1A1*6*, and four were heterozygous for *UGT1A1*6*. No patient harboring the *UGT1A1*28* allele was included.

Twenty-five patients received a median of 4.5 courses (eight sessions) of treatment. Toxic effects occurring during any course of treatment are shown in Table 3. Grade 3 or 4 neutropenia occurred in 11 patients (44%), but only one had febrile neutropenia. Nausea and fatigue were common non-hematologic toxic effects, but most cases were Grade 1 or 2. The dose of irinotecan had to be reduced because of toxicity

Table 3. Toxic effects in the phase II study

	Number of patients				Grade 3 or 4 toxicity (%)
	1	2	3	4	
Hematologic					
Leukopenia	3	11	2	1	12
Neutropenia	1	7	10	1	44
Anemia	4	1	1	0	4
Thrombocytopenia	0	0	0	0	0
Non-hematologic					
Febrile neutropenia	—	—	1	0	4
Nausea	9	9	2	0	8
Vomiting	7	4	1	0	4
Anorexia	7	4	2	0	8
Diarrhea	5	4	1	0	4
Stomatitis	11	1	0	0	0
Fatigue	16	4	1	0	4
Alopecia	10	2	—	—	
Hyperglycemia	0	1	3	0	12

Table 4. Tumor responses in the phase II study

Response	Number of patients	Percentage
Complete response	0	0
Partial response	6	24
No change	12	48
Progressive disease	4	16
Not evaluated	3	12
Total	25	

in nine patients (36%); the dose was reduced during the first or second course in eight of these patients. Treatment was delayed during the first two courses in 12 patients (48%). The reasons for treatment delay were neutropenia or leukopenia in 10 patients, anorexia in 2, diarrhea in 2 and infectious colitis in 1. Tumor response is shown in Table 4. Tumor response was assessable in 22 patients. In the other three patients, tumor response could not be assessed because of early discontinuation of treatment. The objective response rate was 24% (95% confidence interval: 9.4–45.1%) with no complete response and six partial responses.

One patient had multiple metastases to the liver, lung and abdominal lymph nodes. The metastases to the lung and abdominal lymph nodes disappeared after eight and a half courses of treatment. In addition, the liver metastasis shrank and could be resected curatively. The major reasons for treatment discontinuation were progressive disease in 18 patients and toxicity or the patient's refusal to continue treatment in 5.

DISCUSSION

This study evaluated the DLT and MTD of the FOLFIRI regimen in Japanese patients with advanced CRC. Observational *UGT1A1* genotyping and pharmacokinetic analysis were also performed in the phase I part, but these lines of information were not reflected for both patient enrollment and dose escalation. We estimated that the RDs of irinotecan and infusional 5-FU for FOLFIRI in Japanese patients were 180 and 2400 mg/m^2, respectively, similar to the RDs in Western countries (1,15).

The incidence of Grade 3 or 4 neutropenia was higher, but that of diarrhea was lower than the incidences in previous studies conducted in Western countries (Table 3) (1,2). Treatment was frequently delayed because of neutropenia but could be continued after dose reduction. Febrile neutropenia occurred in only one patient in the phase II part. Our results suggest that toxic effects associated with the RD of FOLFIRI as determined in this study were manageable in patients without the *UGT1A1*28* allele.

The doses of irinotecan and infusional 5-FU did not reach the MTD, and only one patient had DLT (Grade 3 diarrhea) at dose Level 2 (irinotecan 150 mg/m^2 and infusional 5-FU 2400 mg/m^2). Therefore, the question remains whether the doses of irinotecan and infusional 5-FU could have been escalated much higher. Previous clinical studies, without *UGT1A1* genotyping, reported that irinotecan could be administered in a dose around 260 mg/m^2. However, these studies did not show a clear advantage of using a higher dose of irinotecan with respect to efficacy and recommended 180–200 mg/m^2 of irinotecan on the basis of toxicity and compliance (15,16).

Although we analyzed *UGT1A1* genotypes, prior stratification had not been applied for dose escalation based on *UGT1A1* genotypes or $AUC_{SN\text{-}38}/AUC_{SN\text{-}38G}$. *UGT1A1* genotyping and pharmacokinetic data were available for 8 of 12 patients who received dose Levels 2 or 3. The patient with *UGT1A1*6/*28* who had Grade 4 neutropenia during the first course could continue FOLFIRI treatment after reducing the dose of irinotecan to 100 mg/m^2. $AUC_{SN\text{-}38}/AUC_{SN\text{-}38G}$ decreased from 2.16 to 1.56 after dose reduction. The patient had a partial response, with no further severe myelosuppression. One patient with *UGT1A1*1/*1* genotype had DLT. Although there was no clear-cut relation between *UGT1A1* genotype and DLT because of the small number of patients, our results suggest that patients harboring *UGT1A1*6/*28* should be cautiously treated with FOLFIRI and dose reduction might be considered. Previous studies have recommended that caution is exercised when patients with *UGT1A1*6/*28*, **6/*6* or **28/*28* receive FOLFIRI (8–10). However, no confirmatory dose adjustment study in this population exists and optimal dose remains to be explored.

A genotype-driven phase I study of irinotecan included in the FOLFIRI regimen given to Western patients without *UGT1A1*28/*28* demonstrated a higher MTD in those with *UGT1A1*1/*1* or *UGT1A1*1/*28* genotype and a dose-dependent tumor response (17). In Japan and other Asian countries, dose escalation studies of irinotecan in FOLFIRI should be performed taking into account *UGT1A1*28* as well as the **6* genotypes, since the RD may be influenced by the presence of these variant alleles (8–10). The RD of irinotecan for patients without *UGT1A1*28/*28*, **6/*6* or **6/*28* might be higher even among Asians. However, we could not plan the genotype-driven phase I study of irinotecan in the FOLFIRI regimen at that time, because there was limited information regarding the effects of *UGT1A1*6* and **28* on the irinotecan-related toxicities.

In the phase II part of this study, we excluded patients who had at least one *UGT1A1*28* allele, because we had considered at that time that these patients were at a higher risk of irinotecan-induced severe toxicities based on the report by Ando et al. (3). So, we demonstrated the feasibility of FOLFIRI at RDs in a limited population.

The RDs of FOLFIRI in Japanese patients were proved to be consistent with those in Western countries. This finding implies that it may be possible for Japanese patients to participate in global trial(s) to evaluate any investigational new agent combined with FOLFIRI.

In conclusion, this phase I/II study demonstrates that the RDs of irinotecan and infusional 5-FU in FOLFIRI for Japanese patients without the *UGT1A1*28* allele are determined to be 180 and 2400 mg/m^2, respectively. Toxic effects at these doses are manageable based on this protocol setting.

Funding

This study was supported in part by the Grant-in-Aid for Cancer Research from the Ministry of Health, Labour and Welfare of Japan [21S-8-1], in part by a Grant-in-Aid for Scientific Research (C) from the Ministry of Education [20590546], Culture, Sports, Science and Technology (MEXT) and in part by a Grant-in-Aid for 'Support Project of Strategic Research Center in Private Universities' from the MEXT, awarded by Saitama Medical University Research Center for Genomic Medicine. The study was presented in part at the ASCO GI symposium, San Francisco, CA, January 29–31, 2006.

Conflict of interest statement

None declared.

References

1. Tournigand C, Andre T, Achille E, Lledo G, Flesh M, Mery-Mignard D, et al. FOLFIRI followed by FOLFOX6 or the reverse sequence in advanced colorectal cancer: a randomized GERCOR study. *J Clin Oncol* 2004;22:229–37.
2. Andre T, Louvet C, Maindrault-Goebel F, Couteau C, Mabro M, Lotz JP, et al. CPT-11 (irinotecan) addition to bimonthly, high-dose leucovorin and bolus and continuous-infusion 5-fluorouracil (FOLFIRI) for pretreated metastatic colorectal cancer. GERCOR. *Eur J Cancer* 1999;35:1343–7.
3. Ando Y, Saka H, Ando M, Sawa T, Muro K, Ueoka H, et al. Polymorphisms of UDP-glucuronosyltransferase gene and irinotecan toxicity: a pharmacogenetic analysis. *Cancer Res* 2000;60:6921–6.
4. Innocenti F, Undevia SD, Iyer L, Chen PX, Das S, Kocherginsky M, et al. Genetic variants in the UDP-glucuronosyltransferase 1A1 gene predict the risk of severe neutropenia of irinotecan. *J Clin Oncol* 2004;22:1382–8.
5. Fujita K, Sasaki Y. Pharmacogenomics in drug-metabolizing enzymes catalyzing anticancer drugs for personalized cancer chemotherapy. *Curr Drug Metab* 2007;8:554–62.
6. Gagne JF, Montminy V, Belanger P, Journault K, Gaucher G, Guillemette C. Common human UGT1A polymorphisms and the altered metabolism of irinotecan active metabolite 7-ethyl-10-hydroxycamptothecin (SN-38). *Mol Pharmacol* 2002;62:608–17.
7. Premawardhena A, Fisher CA, Liu YT, Verma IC, de Silva S, Arambepola M, et al. The global distribution of length polymorphisms of the promoters of the glucuronosyltransferase 1 gene (UGT1A1): hematologic and evolutionary implications. *Blood Cells Mol Dis* 2003;31:98–101.
8. Araki K, Fujita K, Ando Y, Nagashima F, Yamamoto W, Endo H, et al. Pharmacogenetic impact of polymorphisms in the coding region of the UGT1A1 gene on SN-38 glucuronidation in Japanese patients with cancer. *Cancer Sci* 2006;97:1255–9.
9. Han JY, Lim HS, Shin ES, Yoo YK, Park YH, Lee JE, et al. Comprehensive analysis of UGT1A polymorphisms predictive for pharmacokinetics and treatment outcome in patients with non-small-cell lung cancer treated with irinotecan and cisplatin. *J Clin Oncol* 2006;24:2237–44.
10. Minami H, Sai K, Saeki M, Saito Y, Ozawa S, Suzuki K, et al. Irinotecan pharmacokinetics/pharmacodynamics and UGT1A genetic polymorphisms in Japanese: roles of UGT1A1*6 and *28. *Pharmacogenet Genomics* 2007;17:497–504.
11. *Handbook for Recording Results of Cancer Treatment*. Geneva, Switzerland: World Health Organization 1979.
12. Fujita K, Ando Y, Nagashima F, Yamamoto W, Eodo H, Araki K, et al. Genetic linkage of UGT1A7 and UGT1A9 polymorphisms to UGT1A1*6 is associated with reduced activity for SN-38 in Japanese patients with cancer. *Cancer Chemother Pharmacol* 2007;60:515–22.
13. Simon R. Optimal two-stage designs for phase II clinical trials. *Control Clin Trials* 1989;10:1–10.
14. Uemura N, Yamada Y. FOLFIRI regimen for metastatic or recurrent colorectal cancer. *Gan To Kagaku Ryoho* 2006;33:904–6.
15. Ducreux M, Ychou M, Seitz JF, Bonnay M, Bexon A, Armand JP, et al. Irinotecan combined with bolus fluorouracil, continuous infusion fluorouracil, and high-dose leucovorin every two weeks (LV5FU2 regimen): a clinical dose-finding and pharmacokinetic study in patients with pretreated metastatic colorectal cancer. *J Clin Oncol* 1999;17:2901–8.
16. Duffour J, Gourgou S, Desseigne F, Debrigode C, Mineur L, Pinguet F, et al. Multicentre phase II study using increasing doses of irinotecan combined with a simplified LV5FU2 regimen in metastatic colorectal cancer. *Cancer Chemother Pharmacol* 2007;60:383–9.
17. Toffoli G, Cecchin E, Gasparini G, D'Andrea M, Azzarello G, Basso U, et al. Genotype-driven phase I study of irinotecan administered in combination with fluorouracil/leucovorin in patients with metastatic colorectal cancer. *J Clin Oncol* 2010;28:866–71.

0090-9556/11/3902-161–164$20.00
DRUG METABOLISM AND DISPOSITION

DMD 39:161–164, 2011

Vol. 39, No. 2
35451/3657144
Printed in U.S.A.

Short Communication

Delayed Elimination of SN-38 in Cancer Patients with Severe Renal Failure

Received July 13, 2010; accepted October 27, 2010

ABSTRACT:

This prospective study is designed to examine the effects of severe renal failure on the pharmacokinetics of irinotecan. The pharmacokinetics of irinotecan, 7-ethyl-10-hydroxycamptothecin (SN-38), and SN-38 glucuronide (SN-38G) in three cancer patients with severe renal failure [creatinine clearance (Ccr) ≤20 ml/min] who were undergoing dialysis and received 100 mg/m^2 irinotecan as monotherapy were prospectively compared with those in five cancer patients with normal renal function (Ccr ≥60 ml/min). To ensure that the subjects had similar genetic backgrounds of *UDP-glucuronosyltransferase (UGT) 1A1*, patients with *UGT1A1*1/*1*, **1/*6*, or **1/*28* were enrolled. The estimated terminal elimination rate constant of SN-38 in patients undergoing dialysis was approximately one tenth of that in patients with normal renal function (P = 0.025). Approximately 50% of SN-38 was dialyzed with a 2.1-m^2 dialysis membrane, whereas 27% was dialyzed with a 1.5-m^2 membrane. Our results showed that the elimination of SN-38 was significantly delayed in patients with severe renal failure compared with patients with normal renal function. We demonstrated that SN-38 was partly dialyzed.

Introduction

Several lines of evidence have demonstrated that severe renal failure differentially affects drug uptake or efflux transporters and drug-metabolizing enzymes in the liver. Even drugs that are predominantly eliminated by hepatic transport and metabolism can be affected by severe renal failure, leading to unexpected consequences, such as atypical pharmacokinetics and an increased risk of adverse drug reactions. High levels of uremic toxins in such patients are partially implicated in these effects (Nolin et al., 2008).

Irinotecan is extensively metabolized in the liver to an active metabolite, 7-ethyl-10-hydroxycamptothecin (SN-38), by carboxylesterase, which is then conjugated predominantly by liver UDP-glucuronosyltransferase (UGT) 1A1 to form inactive SN-38 glucuronide (SN-38G) (chemical structures; http://www.pharmgkb.org/search/pathway/irinotecan/metabolites.html). Polymorphisms in *UGT1A1* gene, such as *UGT1A1*28* and **6*, can cause reduced glucuronidation of SN-38, thus resulting in severe irinotecan-induced toxicity. *UGT1A1*6/*6*, **28/*28*, and **6/*28* genotypes have been linked to significantly decreased conversion of SN-38 to SN-38G and severe neutropenia in Asians (Minami et al., 2007).

Transporters expressed in the liver are also implicated in the pharmacokinetics of irinotecan and its metabolites. The uptake of SN-38 from the systemic circulation by hepatocytes is mediated by organic anion transporter peptide 1B1 (OATP1B1) (Nozawa et al., 2005). ATP-binding cassette transporters such as ABCC2, ABCB1, and ABCG2 govern the biliary excretion of irinotecan and its metabolites (http://www.pharmgkb.org/do/serve?objId = PA2001&objCls = Pathway).

Because irinotecan is extensively metabolized and transported in the liver, attention has been focused on the hepatic factors underlying interpatient variability in pharmacokinetics of irinotecan. Studies examining the pharmacokinetics of irinotecan in renally impaired patients are scant. The pharmacokinetics of irinotecan in patients with mild renal impairment who had a creatinine clearance (Ccr) of 35 to 66 ml/min were similar to those in patients with normal renal function (de Jong et al., 2008). Although several case reports have examined the effects of more severe renal dysfunction requiring dialysis on the pharmacokinetics or toxicity of irinotecan (Venat-Bouvet et al., 2007; Czock et al., 2009), no prospective study has been performed; nevertheless, such rare patients are given irinotecan in clinical practice.

Therefore, we prospectively examined the pharmacokinetics of irinotecan, SN-38, and SN-38G in cancer patients with severe renal failure who were undergoing dialysis compared with patients with normal renal function. We enrolled patients with *UGT1A1*1/*1*, **1/*6*, or **1/*28* to ensure that the subjects had similar genetic backgrounds of *UGT1A1*.

Materials and Methods

Materials. Irinotecan, SN-38, and SN-38G were purchased from Toronto Research Chemicals (North York, Canada). All chemicals and solvents were of the highest grade commercially available.

Study Design. Patients who were candidates to receive the 100 mg/m^2 irinotecan monotherapy, satisfying the eligibility criteria listed below, were prospectively enrolled in this study. All patients were divided into two groups:

This work was supported in part by the Grant-in-Aid for Cancer Research from the Ministry of Health, Labour and Welfare of Japan [Grant 21S-8-1]; and a grant-in-aid for "Support Project of Strategic Research Center in Private Universities" from the Ministry of Education, Culture, Sports, Science and Technology (to Saitama Medical University Research Center for Genomic Medicine).

Article, publication date, and citation information can be found at http://dmd.aspetjournals.org.

doi:10.1124/dmd.110.035451.

ABBREVIATIONS: UGT, UDP-glucuronosyltransferase; SN-38, 7-ethyl-10-hydroxycamptothecin; SN-38G, SN-38 glucuronide; OATP1B1, organic anion transporter peptide 1B1; Ccr, creatinine clearance; CMPF, 3-carboxy-4-methyl-5-propyl-2-furanpropanoic acid; IA, indoleacetic acid; IS, indoxyl sulfate; HA, hippuric acid; λ_z, terminal elimination rate constant.